

# Battery Electric Vehicle-in-the-Loop Power and Efficiency Measurement Test Method

Philip Rautenberg<sup>1</sup>, Benedikt Reick<sup>2</sup>, Danilo Engelmann<sup>3</sup>, Michael Frey<sup>1</sup>, and Frank Gauterin<sup>1</sup>

<sup>1</sup>Karlsruhe Institute of Technology

<sup>2</sup>Ravensburg-Weingarten University of Applied Sciences

<sup>3</sup>Bern University of Applied Sciences TI

## Abstract

The increasing adoption of battery electric vehicles (BEVs), driven by the EU's target of no internal combustion engine vehicles from 2035 onwards, is driving significant changes in the automotive industry. However, the high degree of electrification and the unique low-speed acceleration behavior of BEVs therefore lead to new challenges. Measuring the drivetrain power and efficiency in a reproducible way and obtaining meaningful results is one of the challenges.

To address this challenge, a novel test method is developed that offers a simple and preferably modification-free approach to drivetrain power and efficiency measurements for BEVs, allowing for efficient and reproducible testing. Different paths for determining the drivetrain power with varied measurement efforts are presented and evaluated. The test method is designed to provide reliable and accurate results for BEVs.

In this study, the effectiveness of the test method is shown by presenting the results of tests conducted with a VW e-up! on a Vehicle-in-the-Loop test bench and comparing them with data from previous studies. The results show that this approach offers a reproducible and meaningful way to measure power and efficiency in BEV's drivetrains.

In addition to the discussion of the results, insights into the measurement of BEV's drivetrains are given. An outlook on future challenges and how to overcome these with the help of the presented test bench as well as the knowledge gained from the study completes the paper.

Overall, the study offers insights into the development and testing of BEVs, providing a robust and reliable test method.

## Introduction

A general procedure for measuring the performance of electric vehicles (EVs) on chassis dynamometers is presented in [1]. The drivetrain of an EV and its specialties like recuperation behavior and the non-disconnectable clutch-free drivetrain is described. Other measuring guidelines for EVs can be found in relevant regulations, see [2,3,4,5].

Chassis dynamometer power measurements allow the calculation of the vehicle motor power based on the measured wheel power. The determined power represents a real-driving power including the influence of tires, transmission, electric components and also the temperature of all relevant components. To ensure high repeatability, an elimination of as many uncertainties as possible without relying on unknown sensors and measurement systems is useful. Wheel hub dynamometers allow to eliminate the influence of the tire [6,7], which provides a high uncertainty in classic roller chassis dynamometers. Wheel hub dynamometers are ideal for determining drivetrain efficiency and maximum power, especially during start-up. Such a setup is used and described in detail for the verification of existing methods as well as for the method's further development.

The purpose of power measurement includes checking unauthorized modifications by test organizations or also deliberate modification in racing. Power measuring also can be used to determine the vehicle efficiency while driving. Roller chassis and wheel hub dynamometers are widely used in companies, universities, and testing institutions.

The studies in this paper verify the validity of the presented method for wheel hub dynamometers. After the general validity of this method can be shown, an extension for wheel hub dynamometers is displayed to increase the accuracy at a manageable effort. Differences between the two types of dynamometers are explained and discussed in detail. The suitability of measuring the efficiency of a vehicle powertrain on a wheel hub test bench is justified.

Based on the collected measuring data, an advanced proposal for a test procedure for EVs is presented. Proposals for further improvement and more detail of the measuring procedure are summarized in conclusion. To investigate the advanced method, a VW e-up! (2019) is tested on a wheel hub dynamometer at the Karlsruhe Institute of Technology.

## Basics on Power and Efficiency Calculation for Electric Vehicles

The calculation of the power as well as the efficiency of an electric drivetrain can be done with the help of different vehicle state variables. An EV with front-wheel drive and a single-speed transmission (SST) is considered in this work, as shown in Figure 1.

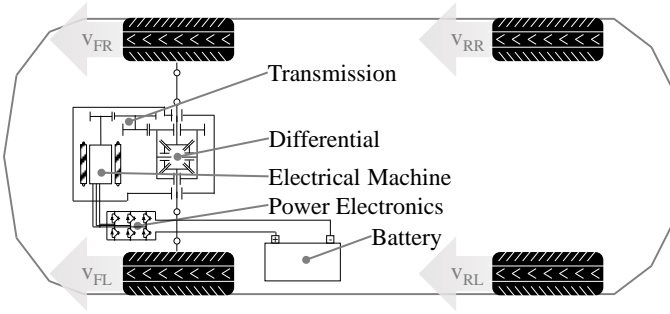


Figure 1. Sketch of an EV with SST.

In addition to the measured vehicle velocity  $v$  and wheel torque  $T_W$ , the power calculation requires knowledge of the dynamic tire radius  $r_{dyn}$ , the ratio  $i$  and the efficiency  $\eta$  of the differential and the transmission.

The dynamic tire radius can be used to determine the wheel speed  $n_W$  from the vehicle velocity:

$$n_W = \frac{v}{2\pi \cdot r_{dyn}} \quad (1)$$

With the wheel speed and the total gear ratio of the transmission  $i_T$  and differential  $i_D$ , the speed of the electric motor (EM)  $n_{EM}$  can be determined in the next step:

$$n_{EM} = n_W \cdot i_T \cdot i_D \quad (2)$$

The mechanical torque at the EM  $T_{EM}$  is calculated using the summed torque at the two front wheels as well as the total ratio and the total efficiency of the transmission and differential  $i_T \cdot i_D$  and  $\eta_T \cdot \eta_D$ :

$$T_{EM} = \frac{T_W}{i_T \cdot i_D \cdot \eta_T \cdot \eta_D} \quad (3)$$

The mechanical power of the EM  $P_{EM,m}$  can then be calculated from the EM's speed  $n_{EM}$  from equation (2) as well as the EM's mechanical torque  $T_{EM}$  from equation (3):

$$P_{EM,m} = 2 \cdot \pi \cdot n_{EM} \cdot T_{EM} \quad (4)$$

If the effective voltage  $U_{AC}$  and the effective current  $I_{AC}$  of the EM's three phases are also available, the angular phase shift  $\cos(\varphi)$  can be obtained. Using this data, the efficiency  $\eta_{EM}$  of the electrical machine can be determined:

$$\eta_{EM} = \frac{P_{EM,m}}{\sqrt{3} \cdot U_{AC} \cdot I_{AC} \cdot \cos(\varphi)} \quad (5)$$

With the knowledge of the EM's speed as well as the EM's phase frequency  $f$ , also the integer pole pair number  $p$  of the EM can be determined:

$$p = \frac{f}{n_{EM}} \quad (6)$$

The efficiency of the power electronics can be calculated with the DC current  $I_{DC}$  as well as the DC voltage  $U_{DC}$ :

$$\eta_{PE} = \frac{P_{EM,el}}{U_{DC} \cdot I_{DC}} = \frac{\sqrt{3} \cdot U_{AC} \cdot I_{AC} \cdot \cos(\varphi)}{U_{DC} \cdot I_{DC}} \quad (7)$$

Since many of the required variables are not necessarily known or are difficult to measure or determine, the following chapters present a method that allows the determination of the motor power as well as the determination of the efficiency even with little prior knowledge.

## Test Environment and Setup

### Conventional Chassis Dynamometers

Conventional chassis dynamometers offer the following testing setups considering longitudinal dynamics [8]:

- Roller dynamometers for emission development and certification
- Roller dynamometers for consumption, efficiency and performance measurements
- Roller dynamometers for endurance and fatigue testing
- Roller dynamometers for noise vibration harshness (NVH) analysis
- Roller dynamometers for electromagnetic compatibility (EMC) analysis

In general, chassis dynamometers can be classified into test systems with tire-to-ground contact and without tire-to-ground contact.

With tire-to-ground contact there are apex roller and prism roller chassis dynamometers, see Figure 2. The reproduction of realistic tire-ground contact is a challenge on these testing systems. In the case of the apex roller system, the tire rolls on the testing roller, creating a linear contact between the roller and the tire on the bottom. The larger the roller diameter, the more realistic the tire-to-ground contact, but the larger the construction space required. As the vehicle needs to be clamped to the ground in this concept, the wheel downforces increase with this testing system. In the case of the prism roller design, the vehicle does not need to be clamped, so the wheel downforces are not modified. In addition, the prism roller requires less construction space. However, this testing rig results in two contact points between the tire and rollers. This in turn leads to less realistic conditions.

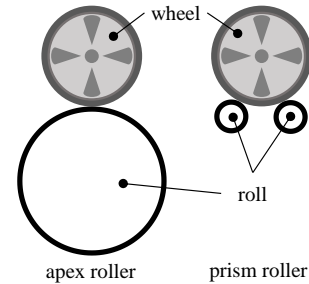


Figure 2. Chassis dynamometer design with tire ground contact. [1] © SAE International

For the most accurate and realistic determination of engine power through measuring wheel power, mastering the tire-to-ground contact in the testing system is essential.

In the case of the apex roller testing system, a formula is known from [9] that corrects the rolling resistance based on the radius ratio between the tire and the testing roller. The rolling resistance on the

dynamometer roller  $F_{R\delta}$  is corrected in comparison to the rolling resistance on the road  $F_R$  by means of the roller diameter  $r_\delta$  and the dynamic tire radius  $r_{\text{dyn}}$  (see equation (8) from [9]). The larger the roller diameter, the closer the contact surface is to an even track due to the lower curvature of the roadway.

$$F_{R\delta} = F_R \cdot \left(1 + \frac{r_{\text{dyn}}}{r_\delta}\right)^{1/2} \quad (8)$$

Vehicles on chassis dynamometers with tire-to-ground contact must be fixed, especially for apex rollers. This is not necessarily done by horizontal fixations. Often, the vehicle is clamped to the ground by chains, both, at the front and at the rear of the vehicle, see Figure 3.

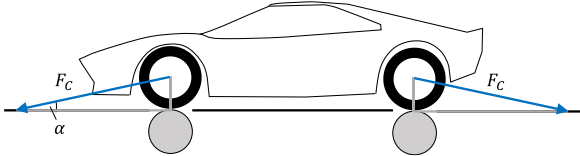


Figure 3. Clamping force on an apex roller dynamometer.

This type of fixation has a direct influence on the rolling resistance, since an additional force presses the vehicle onto the roller. A factor from the clamping force  $F_C$  and the cosine of the clamping angle  $\alpha$  must also be added to the normal force  $F_N$ . This results in an adjustment of equation (8):

$$F'_{R\delta} = (F_N + F_C \cdot \sin(\alpha)) \cdot f_R \cdot \left(1 + \frac{r_{\text{dyn}}}{r_\delta}\right)^{1/2} \quad (9)$$

Chassis dynamometers without tire-to-ground contact are, for example, wheel hub dynamometers. These dynamometers often additionally enable testing of lateral dynamics. In such a test environment, the study of lateral dynamics is enabled by the realistic replication of vehicle dynamics in complex vehicle simulations. [7]

This study focuses on the measurement of longitudinal dynamic efficiency and performance. Showing what advantages a wheel hub dynamometer can deliver compared to classic roller chassis dynamometers is intended.

A detailed description of the considered wheel hub dynamometer is given in the next chapter.

### Vehicle-in-the-Loop Test Bench

Powertrain or wheel hub dynamometers expand the number of investigation options for vehicles and allow influencing factors to be minimized, since the wheels of the Vehicle under Test (VUT) are disassembled and the vehicle is mechanically connected directly to the load machines via the wheel hub. An example of such a test rig is the Vehicle-in-the-Loop full vehicle test bench (ViL) of the Institute of Vehicle System Technology at the Karlsruhe Institute of Technology (KIT-FAST), which is shown in Figure 4.



Figure 4. Mounted VUT at the ViL test bench of the KIT-FAST.

Four permanently excited synchronous machines are each connected to a wheel of the VUT via constant velocity drive shafts and bearing blocks. The load machines are supplied with the correct voltage by dynamic frequency converters depending on the load point. The bearing blocks and constant velocity drive shafts permit different chassis geometries and associated, chassis-specific varying angles (e.g. camber or toe angle). Torque measuring hubs are fitted at the junction between the bearing block and wheel hub on each wheel to measure the torque close to the driveline. The wheel speed is measured directly at the load machines. The load machine's speed can be considered equivalent to the wheel's speed, since homokinetic (constant velocity) drive shafts are installed between the load machines and the wheels, which ensure a steady transition of angular velocities. This enables correct measurement of torque and speed. Figure 5 shows schematically the positions of the various measuring points.

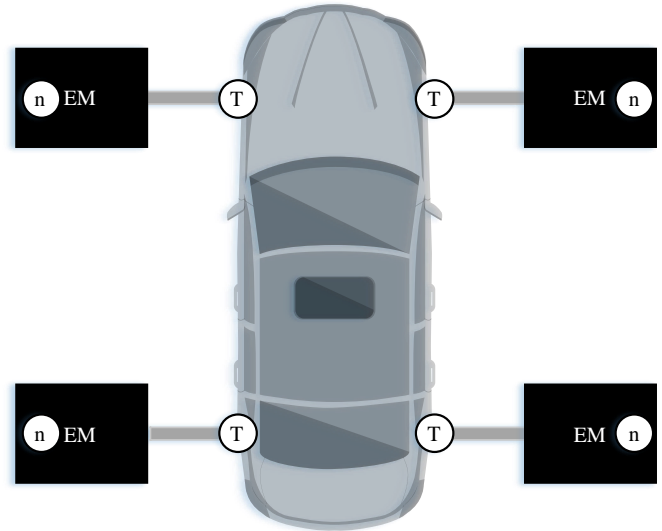


Figure 5. Schematic illustration of the speed (n) and torque (T) measuring points at the ViL.

In addition to the investigation of the longitudinal dynamics of the VUT, investigations during cornering can also be carried out using the software CarMaker from IPG Automotive. The rotatable design of the bearing block and the use of large-angle constant velocity drive shafts enable mechanical steering angles of up to  $20^\circ$  at the wheel without modifications to the steering system. For this purpose, two additional electric motors are mounted on each front wheel, which can emulate the aligning torque on the front wheels via chain drives, see Figure 6.

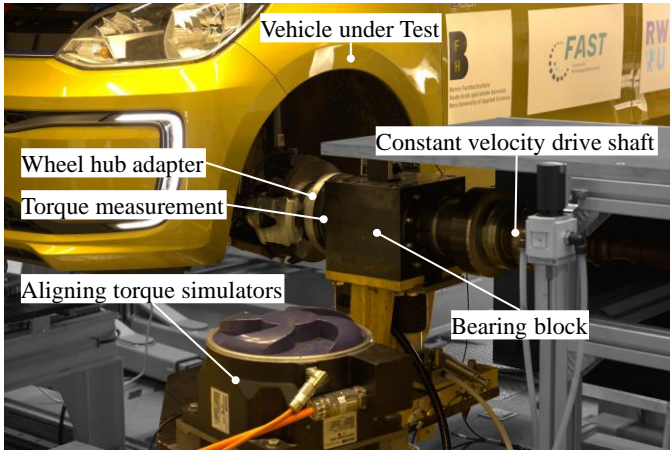


Figure 6. Aligning Torque simulator at the left front wheel.

The test stand is controlled by an automation system, which is implemented via a real-time system with a control and measuring frequency of up to 2 kHz. Communication takes place via EtherCAT or CAN. With the help of the automation, torque or speed controls can be realized and standardized test procedures (e.g. Worldwide harmonized Light-duty vehicles Test Procedure) can be run.

The technical data of the test bench and for possible VUT's are listed in Table 1. Further information about the test bench and especially the driving robotics used for testing, consisting of a pedal and a steering robot, can be taken from [7].

Table 1. Technical data of the test bench.

Description	Unit	Data
Nominal wheel load power	kW	209
Max. wheel load torque at nom. speed (800 rpm)	Nm	2500
Max. wheel speed	rpm	2000
Max. self-aligning torque at the front wheels	Nm	1000
Max. steering angle at the front wheels	deg	±20
Max. air fan speed	km/h	135
Max. vehicle weight	kg	12000
Max. wheel load	kg	3000
Wheelbase	m	1.8 – 4.9
Track width	m	1.2 – 3.9

### Comparison of the Test Environment Concepts

The various test bench concepts differ in the suitability for measuring the VUT's powertrain. When comparing the two test bench concepts with each other and additionally with tests of the entire vehicle on real roads, the advantages and disadvantages become apparent. The focus of the powertrain investigation in this study is on the torque of the electric motor. To determine the torque, the vehicle's technical data on the differential and transmission ratios are required. This applies to all three test methods. However, the accuracy of the torque determination due to various influences in the measurement accuracy varies depending on the test case, as shown in Figure 7.

In all three methods, the sensor technology is based on basic physical principles. The accuracy can therefore be considered as comparable. For details on different measuring principles, please refer to [10].

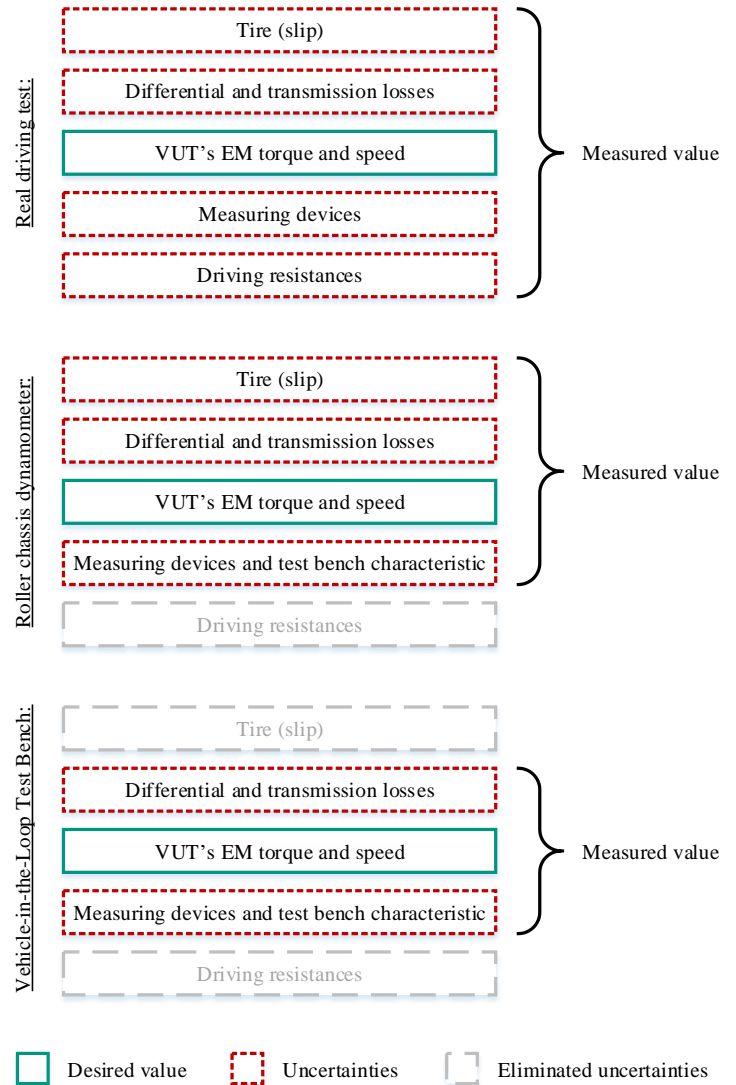


Figure 7. Influencing factors on the torque measurement for the three different test methods.

When testing on real roads, not only vehicle-specific factors such as tire slip or the efficiency of the differential and transmission, but also the driving resistances that cannot be eliminated and the measurement technology have an influence on the accuracy of the torque measurement.

If the test is performed on a roller chassis dynamometer, at least the driving resistances can be eliminated as an influencing factor, so that the accuracy increases. Influences due to the test bench characteristics, such as varying roller diameters or additional rolling resistance due to fixation of the VUT in vertical direction, are indirectly reflected in the measurement technique. The influence on the rolling resistance due to the fixation of the vehicle increases with increasing clamping force  $F_C$  as well as with increasing clamping angle  $\alpha$  according to equation (9). An overview of the relative increase in the rolling resistance due to the fixation for the considered VUT is given in Figure 8. The clamping angle depends on various influencing factors. If the test space is large, the fixations can be clamped over a long distance so that small angles are achieved. At the same time, vehicles with a small ground distance (small or sports cars) can also be fixed with smaller angles, as the anchor point is lower than for vehicles with a large ground distance

(e.g. SUVs). Accordingly, the increase in the rolling friction varies depending on the overall setup.

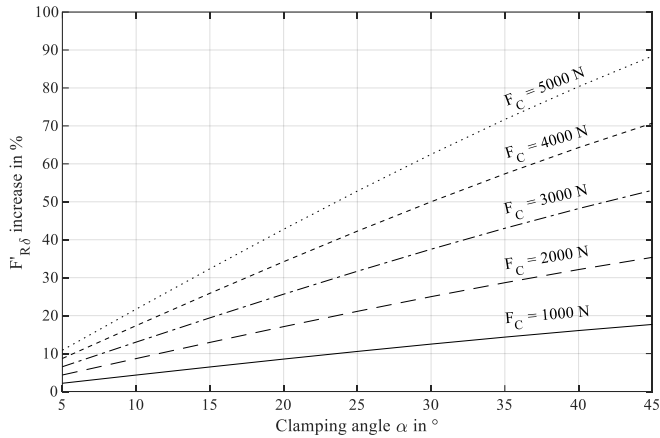


Figure 8. Relative increase in the rolling resistance  $F'_{RD}$  for the considered VUT as a function of the clamping force  $F_C$  and the clamping angle  $\alpha$ .

Finally, if a test bench like the ViL is used, the influence of the tire losses including the tire slip can be eliminated. This can be achieved by the positive connection between the wheel hub, the constant velocity drive shaft and the load machine. A disadvantage is the necessity of special adapters for mounting the VUT. Depending on the bolt circle and diameter of the hub bore, vehicle-specific adapters must be manufactured, see Figure 9. In comparison to the roller chassis dynamometer, there is no influence of rolling friction or clamping forces on the ViL.



Figure 9. Rendering of the wheel hub adapter for mounting the VUT at the ViL.

The highest accuracies are expected when testing on a test bench like the ViL because of the elimination of major uncertainties (tire and driving resistances). Further gains in accuracy can only be achieved either on component test rigs or by minimizing the influence of the measurement technology.

### Vehicle under Test

The investigations were carried out with a battery-electric series production vehicle (BEV) from Ravensburg-Weingarten University of Applied Sciences (RWU). The considered vehicle is a VW e-Up! from 2019, shown on the ViL in Figure 4. The vehicle characteristics relevant to this study are listed in Table 2. A more detailed description of the powertrain can be found in [11].

Table 2. Data of the VUT (VW e-up!).

Variable	Value	Unit	Info
From literature			
$P_{EM,max}$	61	kW	Max. motor power [11]
$T_{EM,max}$	210	Nm	Max. motor torque (up to 2800 rpm) [11]
$n_{EM,max}$	10000	rpm	Max. motor speed [11]
$i_T \cdot i_D$	8,16	-	Total drivetrain ratio [11]
$r_{dyn}$	0.29	m	Dynamic rolling radius of 185/50R16 tire [12]
Measured data			
$m_V$	1354	kg	Curb weight (with driver)

In addition to the vehicle's internal CAN interface, a power meter (PM) was also integrated, which provides the voltages and currents in the DC circuit and the three-phase AC current as measured variables. The PM's setup in the VUT is shown in Figure 10.

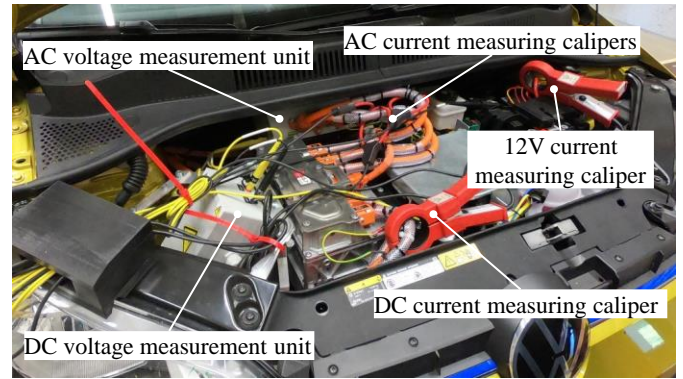


Figure 10. Measurement setup of the PM in the VUT.

## Test Procedures

As shown in previous studies, the power measurement methods depicted in Figure 11 are generally possible to apply on BEVs. The following chapter summarizes the results of the investigation from [1]. Furthermore, an evaluation of these results will be carried out based on the new insights gained from the present study.

### State of the Art

The state of the art presented in [1] highlights the following challenges in the field of power measurement for BEVs.

In roller dynamometers, the high starting torque of BEVs leads to increased tire slip, which complicates the calculation of motor power or requires strong clamping of the vehicle. Ideally, the slip should be determined using additional sensors, but without precise knowledge of the tires and corresponding loss models, a high-quality statement is difficult to make.

The dynamic measurement method from Figure 11 a) is particularly challenging for BEVs as they do not have a starting clutch. The unknown mass inertia must be considered in this dynamic measurement process. Determination of inertia would be possible in principle, but is often technically not feasible as the vehicle would have to be shifted into a neutral gear, which means that the electric machine is disconnected and not running in generator mode.

The neutral gear in BEVs represents a software gear. Many manufacturers still recuperate with low to medium power in this gear, making the determination of the real drivetrains drag losses while driving the vehicle on the roller dynamometer difficult, as the drive also consumes power that is used to generate electrical energy. As a result this also distorts the determination of the inertia and increases the measured drag loss power. If CAN-bus data on the generated electrical power or the mechanical power at the electric machine are known, the drag loss power and inertia can be estimated. Otherwise, additional measuring devices as shown in Figure 10 are necessary.

### Latest Findings

The latest findings from the present investigation lead to the following conclusions.

The disadvantages mentioned negate the time gain from using the dynamic test method (Figure 11 a)). Implementing the static method c) is more attractive as inertia does not affect the measured power. In practice, it has been found to be useful to first statically accelerate the vehicle in drag mode and then gradually reduce the speed under full load. By starting the power measurement at high vehicle speeds, the electric drivetrain reaches thermal limits later, which should be avoided to determine the maximum power.

The quasi-static method b), which represents a compromise between a) and c), offers little advantages in practice because uncertainties due to an unknown inertia affect the measurements as in method a). The time gain during the measurement is minimal or non-existent because measurements may need to be repeated if the vehicle has to reduce its maximum power due to high temperatures in the inverter or electric motor. In method c), individual static points can be measured later if the system has cooled down in such cases.

If undesired effects such as derating occur, methods a) and b) must always be fully repeated. With method c) only the static load points at which derating has already started need to be repeated. Thus, the time saved in test repetitions is lower with method c) compared to a) and b).

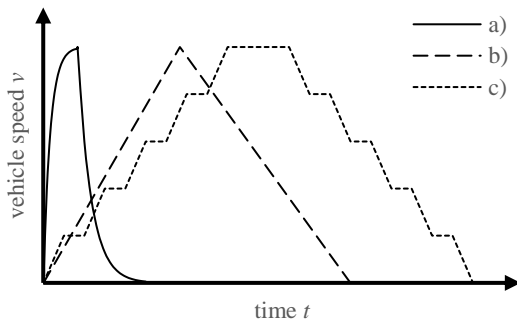


Figure 11. Possible power measuring test methods according to [1] a) dynamic, b) quasi-static and c) static. © SAE International

### Applied Test Procedure

In this study, method c) from Figure 11 for tests is applied due to the previously mentioned reasons. To avoid derating at high powers, method c) is slightly adapted so that the drag power was measured first following the full load power. Accordingly, the vehicle velocity is ramped up in steps (10, 30, 50, 80, 100, and 130 km/h) in neutral gear and the respective speed is always maintained for at least ten seconds. When the highest speed step is reached, the speed is then reduced stepwise (130, 100, 80, 50, 30, and 10 km/h) and held for at least ten

seconds each time with gear D engaged and the accelerator pedal being fully pressed to measure the maximum power available.

In the performed tests, various vehicle variables were measured, which are used for the subsequently presented calculation methods. Basically, a distinction must be made between the test bench, the vehicle and the external measurement technology. Table 3 gives an overview of the measured quantities.

The test bench measurement technology provides wheel-specific speeds and torques. The speeds are converted to an averaged wheel speed  $n_W$ . The torques of the driven wheels are summed to give a total torque  $T_W$ . The position of the measuring points on the test bench are shown in Figure 5.

Different EM powers, the DC link's voltage and current as well as the vehicle velocity are provided via the vehicle's internal CAN interface.

With the PM from Figure 10, the DC link's voltage and current as well as the EM's phase frequency can also be measured. As the inverter efficiency is not the main focus in this investigation, the also measured AC power is not considered.

Table 3. Measurement values of the presented study.

Variable	Unit	Source	Description
$T_W$	Nm	ViL	Summed torque of the actuated wheels
$n_W$	rpm	ViL	Averaged speed of the wheels
$P_{EM,m}$	kW	CAN	Mechanical power of the VUT's EM
$P_{EM,el}$	kW	CAN	Electrical power of the VUT's EM
$U_{DC}$	V	CAN	DC link voltage of the VUT
$I_{DC}$	A	CAN	DC link current of the VUT
$v$	km/h	CAN	Vehicle velocity
$U_{DC}$	V	PM	DC link voltage of the VUT
$I_{DC}$	A	PM	DC link current of the VUT
$f$	Hz	PM	Phase frequency of the VUT's EM

Various approaches exist for determining the power and efficiency of the EM used based on the equations (1) - (7) and the existing vehicle parameters from Table 2. There are differences, for example, in the number of measurement techniques required or in the accuracy.

### Determination of Drivetrain Power

#### Variant 1.1 – Determination via the Test Bench Measurement Data:

To determine the motor power, equations (2) and (3) are substituted into equation (4):

$$P_{EM,m} = 2 \cdot \pi \cdot n_W \cdot \frac{T_W}{\eta_T \cdot \eta_D} \quad (10)$$

Since the efficiencies for the transmission and the differential are unknown, assumptions are required here. Based on the VDI guideline 2157 [13] and the knowledge about the use of an SST, standard values can be assumed for the efficiencies. Table 4 lists various gear efficiencies as well as bearing efficiencies.

Table 4. Efficiencies for gears and bearings according to the VDI guideline 2157 [13].

Description	Efficiency
Outside-outside toothing	0,99
Outside-inside toothing (not relevant for standard SST)	0,995
Bearings	0,995

Since both the transmission and the differential consist of bearings and gears, the following equation (11) can be established for both components:

$$\eta_T \cdot \eta_D = \eta(i, j) = 0,99^i \cdot 0,995^j \quad (11)$$

Since there is no slip at both driven VUT's wheels on the ViL, the differential transmits the torque of the EM equally to both wheels. This results in less tooth engagements in the differential. Accordingly, the differential can be simplified and considered as a shaft with one gear. The simplified differential and the remaining tooth engagements in the drivetrain are shown in Figure 12. In addition, the figure shows the positions of the bearings in the drivetrain. The losses of the motor shaft bearings (blue circles) can be considered as losses of the EM. The remaining bearings (green circles), including wheel bearings, are included in the losses, which are to be determined with the use of the VDI guideline 2157 [13]. Accordingly, the following values result for the number of bearings and tooth engagements:

$$i = 2, \quad j = 6$$

The mechanical power of the EM from equation (10) can then be determined using the test bench's measured variables for speed and torque at the wheels.

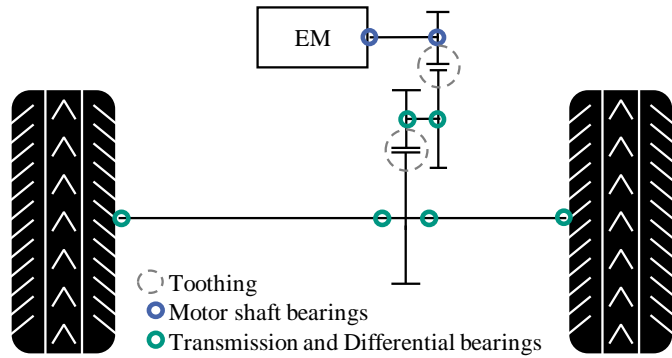


Figure 12. Positions of bearings and tooth engagements in the VUT's drivetrain for the assumption of efficiencies according to VDI guideline 2157 [13].

To determine the motor torque, equation (3) is applied using the same approach as before:

$$T_{EM,m} = \frac{T_W}{i_T \cdot i_D \cdot \eta_T \cdot \eta_D} \quad (12)$$

With this variant, the speed as well as the mechanical torque and the mechanical power at the wheel and at the EM can thus be determined.

However, the assumption of the relative efficiencies via the VDI guideline 2157 [13] is not used for the drag power test phase, since the transmission's and differential's efficiencies are expected to be smaller in this low power phase.

### Variant 1.2 – Determination via the Vehicle CAN Data:

The vehicle's internal CAN interface provides the engine power directly as a measured variable, see Table 3. For determining the motor characteristic field, however, the torque is missing. This can be determined by converting and combining equations (1), (2) and (4):

$$T_{EM,m} = \frac{r_{dyn} \cdot P_{EM,m}}{v \cdot i_T \cdot i_D} \quad (13)$$

However, the vehicle's internal CAN interface does not provide the drag losses of the drivetrain, neither for the drag phases nor for drive phases.

### Variant 1.3 – Combining Vehicle CAN Data and Test Bench Measurement Data:

By combining different measurement techniques, the drag power or drag torque can be determined, both for drag phases and for drive phases.

The drag power can be calculated by subtracting the wheel power with the mechanical power provided via the CAN bus:

$$P_{Drag} = P_W - P_{EM,m} \quad (14)$$

The wheel power or idealized EM power is calculated from the test bench measurement data for wheel speed and wheel torque:

$$P_W = 2 \cdot \pi \cdot n_W \cdot T_W \quad (15)$$

The drag torque can be determined by subtracting the wheel torque of the test bench measurement data with the mechanical torque determined via CAN data from equation (13):

$$T_{Drag} = T_W - T_{EM,m} \quad (16)$$

### Determination of Drivetrain Efficiency

#### Variant 2.1 – Determination via the Test Bench Measurement Data and the Power Meter Data:

Additional external measurement technology for measuring the DC link's voltage and current allows the electric components efficiency to be determined by combining equations (5) and (7). For this, the mechanical power of the EM determined in equation (10) is used:

$$\eta_{PE} \cdot \eta_{EM} = \frac{P_{EM,mech}}{U_{DC} \cdot I_{DC}} \quad (17)$$

In this case, however, not only the determination of the EM's efficiency, but also the determination of the power electronics' (PE) efficiency is carried out, since the measured quantities used for voltage and current were measured at the DC link - between battery and PE.

#### Variant 2.2 – Determination via the Vehicle CAN Data:

The vehicle's internal CAN interface already supplies various variables for the mechanical power and the electrical power, as well as additionally the voltage and the current in the DC link. The two powers can be used to determine the efficiency of the EM:

$$\eta_{EM} \cdot \cos(\varphi) = \frac{P_{EM,m}}{P_{EM,el}} \quad (18)$$

The ratio of electrical power and the DC power, which is calculated by multiplying the DC voltage and DC current, can additionally be used to determine the efficiency of the PE:

$$\eta_{PE} = \frac{P_{EM,el}}{U_{DC} \cdot I_{DC}} \quad (19)$$

However, the efficiency of the transmission and differential cannot be determined from the CAN data.

### Variant 2.3 – Determination via the Test Bench Measurement Data and the Vehicle CAN Data:

By combining the CAN data as well as the test bench measurement data, the efficiency of the transmission and differential can additionally also be determined, including for drag and drive phases. This is determined by the ratio of mechanical power at the wheels as well as the mechanical power at the EM:

$$\eta_T \cdot \eta_D = \left( \frac{P_{EM,m}}{P_{Wheel}} \right)^x \quad (20)$$

The variable  $x$  must be varied depending on whether the drag or drive phase efficiency is to be determined:

$$x = \begin{cases} -1, & \text{Drive phase} \\ 1, & \text{Drag phase} \end{cases}$$

## Results

Applying the methods presented for the determination of the drivetrain power and efficiency to the measurement data from the tests with the VUT on the ViL and comparing them with data from measurements on a roller chassis dynamometer [1] shows the following results. For better comparability, the chapter is divided between the determination of drivetrain power and efficiency in the same way as the previous chapter.

### Determination of Drivetrain Power

First, the motor power is plotted against the motor speed in Figure 13 and the motor torque against the motor speed in Figure 14. Both figures include:

- the EM map of the VUT from [11] (EM map),
- the wheel power measured on the ViL test bench ( $P_W$ ) and the mechanical torque at the EM without considering losses ( $T_{EM,m,loss-free}$ ),
- the mechanical EM power and EM torque of the VUT ( $P_{EM,m}$  and  $T_{EM,m}$ ) calculated according to equations (10) and (12),
- and the mechanical EM power ( $\underline{P}_{EM,m}$ ) provided via the CAN bus as well as the mechanical EM torque of the VUT ( $\underline{T}_{EM,m}$ ) calculated according to equation (13).

For the measured quantities  $P_W$  as well as  $\underline{P}_{EM,m}$ , the drag powers are shown in addition to the full load points. Figure 14 also shows the

torque characteristic from a measurement on a roller chassis dynamometer (Roller dyno) from [1].

The measured powers and torques at the ViL correspond to the EM map from [11]. According to this, the EM map already includes the losses via the transmission and the differential, respectively. By comparing the values of  $P_{EM,m}$  with the CAN bus data, the assumption of the efficiencies via the VDI guideline 2157 [13] according to variant 1.1 can be confirmed for the most part. Questionable remains the assumption at low speeds or powers. Here a deviation is evident. Including equation (13), however, the values for the mechanical torque in the CAN bus data for low speeds are high. Assuming a lower torque, the power would also be lower and thus converge back to the data of variant 1.1.

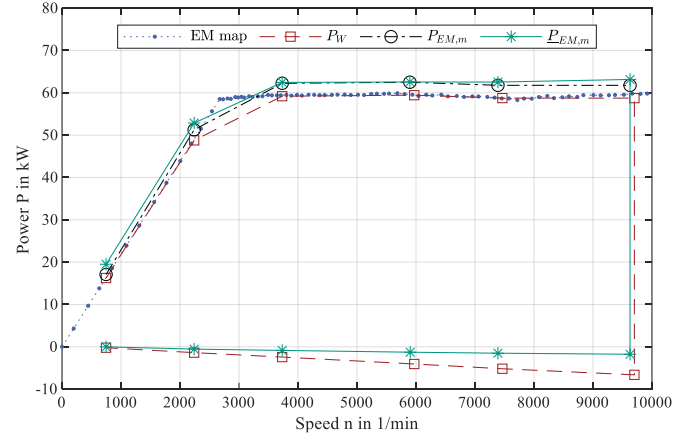


Figure 13. Results for the EM's power over the EM's speed.

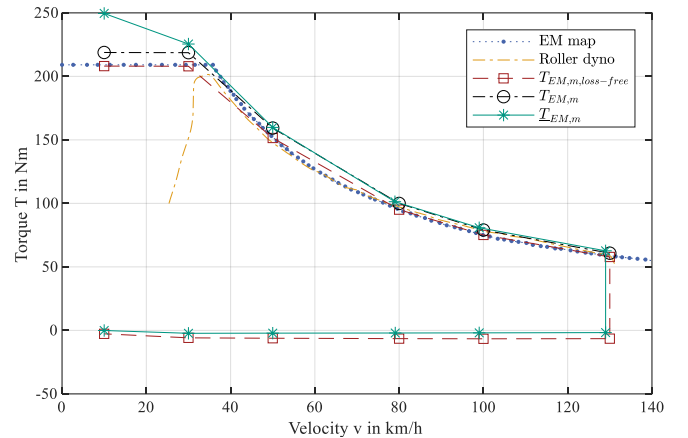


Figure 14. Results for the EM's torque over the vehicle velocity.

Figure 15 additionally shows a detail from Figure 14. This indicates that the motor map can be determined more precisely by testing on the ViL. On the one hand, the full torque can be obtained right from the start, which could lead to spinning wheels or large slip on a roller chassis dynamometer. Secondly, the measured values are significantly closer to the published characteristic curve for motor torque. The cut-off speed was not reached by the ViL measurement because the speeds were sampled in comparatively large steps.

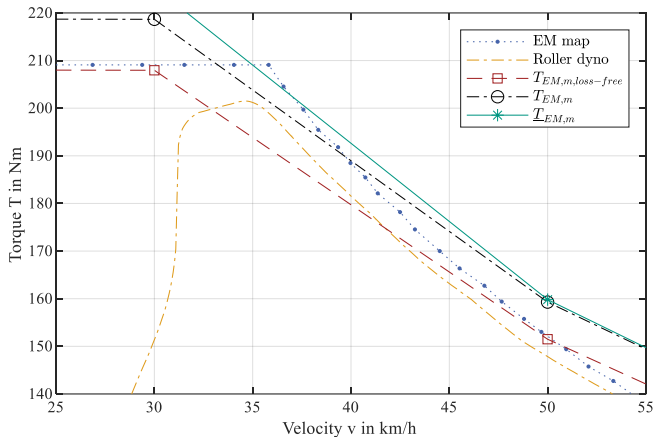


Figure 15. Zoom view of the results for the EM's torque over the vehicle velocity.

Figure 16 shows the drag power in the driving phase and in the drag phase, respectively, according to equation (14). The power in the drag phase has a linear behavior, making the losses increasing with speed obvious. For high speeds, the drag power in the driving phases is comparable. However, at low speeds a deviation from the power in the drag phases is apparent, as the efficiency of gears drop at low speeds and high torques due to less lubrication.

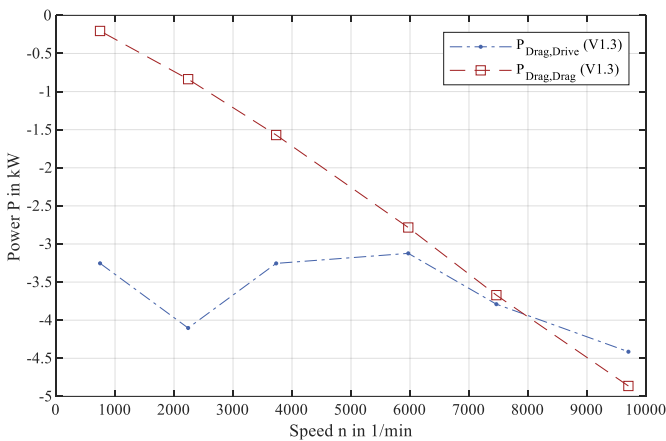


Figure 16. Results for the EM's drag power over the EM's speed from variant 1.3.

### Determination of Drivetrain Efficiency

To analyze the efficiencies, the following two figures show different curves according to calculation variants 2.1-2.3 for driving (Figure 17) and drag phases (Figure 18). In both figures, the efficiencies of EM  $\eta_{EM}$  and PE  $\eta_{PE}$  from equations (18) and (19) of the CAN data are shown, as well as the data from equation (20) for the efficiencies of the transmission and the differential  $\eta_{T+D}$ . In the driving phase, the efficiency of the entire drivetrain  $\eta_{D+T+EM+PE}$  is also shown according to equation (17).

In the driving phase, the PE efficiency calculated from the CAN bus data is noticeable to be greater than 100 %. Although the PE efficiency is normally close to 99 %, exceeding is not plausible. However, calculation errors can occur due to inaccurate current sensors, for example, which can also cause the efficiency to exceed 100 %. Beyond that, however, the remaining efficiencies are plausible. An overall efficiency of the powertrain between 67 and 90 % is realistic.

The assumptions' verification for the efficiencies of the transmission and the differential according to VDI guideline 2157 [13] can also be confirmed here for the load points with a speed greater than 1000 1/min. According to the assumption, the efficiency for both components together is approximately 95 % over the entire speed range. The efficiency according to variant 2.3, apart from the lowest load point, is between 92 and 95 %.

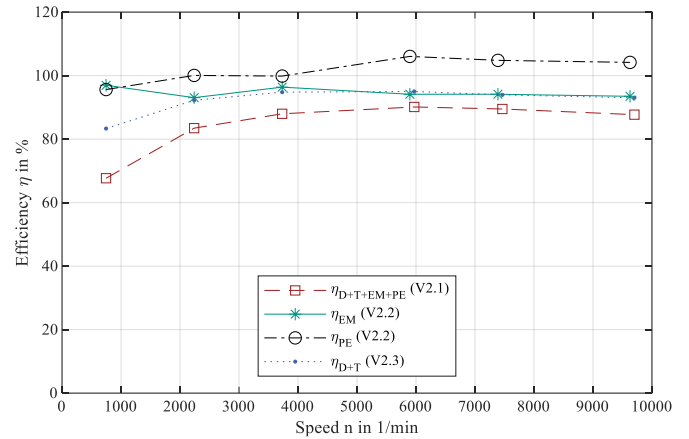


Figure 17. Results for the EM's efficiency over the EM's speed in the drive phases.

In the drag phases, the EM reaches an efficiency of more than 100 % at one load point, see Figure 18. Again, this is not plausible. Furthermore, no plausible efficiencies for the EM and PE can be calculated for the load point with the lowest speed via the CAN bus data, since the electrical power provided by the CAN bus is zero.

The efficiency of the transmission and the differential according to variant 2.3 confirms that the assumptions from variant 1.1 cannot be applied to drag phases.

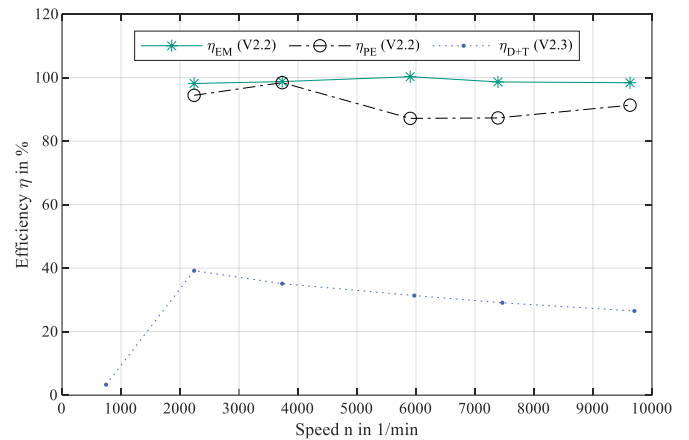


Figure 18. Results for the EM's efficiency over the EM's speed in the drag phases.

### Discussion

The measurement and calculation results are mostly consistent and are within an acceptable range. However, the quality of the CAN bus data must be questioned. The high torque at the lowest load point seems implausible, and so is an efficiency of the PE in driving phases of over 100 %. The plausibility of the data can also not be checked because the

CAN interface does not show which quantities are measured, which are calculated or which are possibly only estimated. For example, a mechanical power of the EM can generally not be measured, but calculated from speed and torque. However, this would require additional torque measurement technology on the rotor or the drive shaft. Additional measurement technology is not practicable for several reasons, e.g. cost, which is why an estimation of the torque via the voltages and currents in the EM in combination with a stored efficiency map must be assumed at this point. For this reason, the use of CAN bus data must always be treated with caution and critically scrutinized. Apart from that, the availability of CAN bus data in BEVs is not mandatory by regulation. Therefore, the assumption should always be that no CAN data is available.

Likewise, the measurement data of the test bench measurement technology as well as the additional measurement technology attached to the vehicle (power meter) must be questioned. However, sufficient accuracy can be assumed for both, since on the one hand purchased measurement systems such as the power meter are usually calibrated and on the other hand the test bench measurement technology is checked regularly.

However, the measurement results show that the assumptions of transmission and differential efficiencies according to VDI guideline 2157 [13] are promising. Only for low speeds the assumption cannot be completely confirmed. Furthermore, the determination of the EM characteristic field with a wheel hub test bench such as the ViL is many times more accurate than with a roller chassis dynamometer. This only requires the knowledge about the ratio of the transmission and the differential in addition to the measured wheel torque and wheel speed.

The adaptation of the static method c) for determining the individual load points from Figure 11 was also appropriate. By determining the drag power first and then determining the full load curve from high speeds to low, derating and thus the repetition of individual load points could be avoided.

## Conclusions and Outlook

The methods presented in this paper for the modification-free approach of measuring BEVs and calculating the performances and efficiencies with varied measurement efforts are proven to be applicable and extend the already existing measurement procedures of BEVs. To fully validate the methods, additional vehicles would need to be tested. Furthermore, the assumption of efficiencies via VDI guideline 2157 [13] would also need to be tested again with other transmission or differential types. If further tests are carried out with BEVs, an assumption for the efficiencies at low speeds could possibly also be developed in this way.

A comparable approach to approximate the motor power of EV's with low measurement effort and without tire slip has not yet existed. This approach will be relevant in the future due to the lack of availability of vehicle data.

In general, this method is not only applicable to series or close-to-series vehicles. The ViL could also be used to test a powertrain without a chassis. In this case, only a mechanism for suspending the components would have to be integrated.

## References

1. Reick, B., Kaufmann, A., and Engelmann, D., "Test Procedure Proposal for EV Power Measurement on Dynamometers", SAE Technical Paper 2021-24-0104, 2021, doi: [10.4271/2021-24-0104](https://doi.org/10.4271/2021-24-0104).
2. ECE/TRANS/WP.29/2020/127, Proposal for Amendment 6 to UN Global Technical Regulation (UN GTR) No. 15 (Worldwide harmonized Light vehicles Test Procedures (WLTP)), Geneva. 182<sup>nd</sup> session, 2020
3. SAE J1634, "Battery Electric Vehicle Energy Consumption and Range Test Procedure", SAE International, 2017, doi: [10.4271/J1634\\_201707](https://doi.org/10.4271/J1634_201707).
4. El Baghdadi, M. et al., "Electric Vehicle Performance and Consumption Evaluation", 2013 World Electric Vehicle Symposium and Exhibition (EVS27), Barcelona, Spain, 2013, pp. 1-8, doi: [10.1109/EVS.2013.6914988](https://doi.org/10.1109/EVS.2013.6914988).
5. Rassölkín, A. and Vodovozov, V., "A test bench to study propulsion drives of electric vehicles," 2013 International Conference-Workshop Compatibility And Power Electronics, Ljubljana, Slovenia, 2013, pp. 275-279, doi: [10.1109/CPE.2013.6601169](https://doi.org/10.1109/CPE.2013.6601169).
6. Gießler, M., Rautenberg, P. and Gauterin F., "Consumption-relevant load simulation during cornering at the vehicle test bench VEL", In: Bargende M., Reuss HC., Wagner A. (eds) 20. Internationales Stuttgarter Symposium. Proceedings. Springer Vieweg, Wiesbaden, 2020, doi: [10.1007/978-3-658-30995-4\\_19](https://doi.org/10.1007/978-3-658-30995-4_19).
7. Rautenberg P., Kurz C., Gießler M. and Gauterin F., "Driving Robot for Reproducible Testing: A Novel Combination of Pedal and Steering Robot on a Steerable Vehicle Test Bench", *Vehicles* 4, no. 3: 727-743, 2022, doi: [10.3390/vehicles4030041](https://doi.org/10.3390/vehicles4030041).
8. Düser, T. et al., „Vehicle Chassis Dynamometers – From certification through to a mechatronic development platform“, München, Süddeutscher Verlag onpact GmbH, 2011.
9. Paulweber, M. and Lebert K., „Mess- und Prüfstandstechnik: Antriebsstrangentwicklung Hybridisierung Elektrifizierung“, Wiesbaden, Springer Vieweg, 2014, doi: [10.1007/978-3-658-04453-4](https://doi.org/10.1007/978-3-658-04453-4).
10. Tränkler, HR. and Reindl, L., „Sensortechnik: Handbuch für Praxis und Wissenschaft“, Heidelberg, Springer Vieweg Berlin, 2015, doi: [10.1007/978-3-642-29942-1](https://doi.org/10.1007/978-3-642-29942-1).
11. Jelden, H., Lück, P., Kruse, G. and Tausen, J., "Der elektrische Antriebsbaukasten von Volkswagen", MTZ Motortechnische Zeitschrift 75, pp. 14-21, 2014, doi: [10.1007/s35146-014-0032-2](https://doi.org/10.1007/s35146-014-0032-2).
12. European Tyre and Rim Technical Organisation (ETRTO), Standards Manual, 2021.
13. VDI 2157, "Planetary gear drives - Definitions, symbols, designs, calculations", VDI-Gesellschaft Produkt- und Prozessgestaltung, 2012.

## Contact Information

M. Sc. Philip Rautenberg  
Karlsruhe Institute of Technology (KIT)  
Institute of Vehicle System Technology (FAST)  
[philip.rautenberg@kit.edu](mailto:philip.rautenberg@kit.edu)

## Definitions/Abbreviations

<b>AC</b>	Alternating current
<b>BEV</b>	Battery electric vehicle
<b>CAN</b>	Controller Area Network
<b>DC</b>	Direct current
<b>EM</b>	Electric motor
<b>EMC</b>	Electromagnetic compatibility
<b>EtherCAT</b>	Ethernet for Control Automation Technology
<b>EV</b>	Electric vehicle
<b>FAST</b>	Institute of Vehicle System Technology
<b>KIT</b>	Karlsruhe Institute of Technology
<b>NVH</b>	Noise vibration harshness
<b>PE</b>	Power electronics
<b>PM</b>	Power meter
<b>RWU</b>	Ravensburg-Weingarten University of Applied Sciences
<b>SST</b>	Single-speed transmission
<b>SUV</b>	Sport Utility Vehicle
<b>VDI</b>	Verein Deutscher Ingenieure
<b>ViL</b>	Vehicle-in-the-Loop
<b>VUT</b>	Vehicle under Test